

Closed-Shell Ion Pairs: Cation and Aggregate Dynamics of Tetraalkylammonium Salts in an Ion-Pairing Solvent

Huaping Mo, Anping Wang,[†] Patricia Stone Wilkinson,[‡] and Thomas C. Pochapsky*

Contribution from the Department of Chemistry, Brandeis University, Waltham, Massachusetts 02254-9110

Received July 11, 1997. Revised Manuscript Received September 26, 1997[⊗]

Abstract: Tetrabutylammonium ion (**1**) forms tight ion pairs with small anions (Cl^- , BH_4^-) in CDCl_3 solution. These ion pairs aggregate as a response to increasing solution concentration with little temperature dependence. Maximum aggregate size is approximately four ion pairs, as measured by comparing self-diffusion coefficients of the aggregates with that of an internal nonaggregating standard of the same shape and nominal size, tetrabutylsilane (**2**). The magnitudes of steady state interionic $^1\text{H}\{^1\text{H}\}$ NOEs observed between **1** and the BH_4^- anion in CDCl_3 as a function of temperature in solutions of fixed concentration are well fit to the standard theoretical expression by assuming a single aggregate size that is independent of temperature. A simplified model-free analysis was applied to steady state $^{15}\text{N}\{^1\text{H}\}$ NOE and ^{15}N T_1 measured at several magnetic field strengths, using ^{15}N -labeled **1** to obtain estimates for reorientational correlation times for the ion aggregates. A similar analysis of $^{13}\text{C}\{^1\text{H}\}$ NOE and ^{13}C T_1 gives local effective correlation times for C–H bond vectors of the 1- CH_2 carbon of **1** and order parameters relating the local motion to overall cation motion. Comparison of these correlation times with those obtained from analysis of $^{29}\text{Si}\{^1\text{H}\}$ NOE, $^{13}\text{C}\{^1\text{H}\}$ NOE, and ^{13}C T_1 for silane **2** provides an estimate of aggregate size which is independent of that obtained by diffusion, with good agreement between the different approaches.

Introduction

Ion pairing is a phenomenon of considerable interest to physical scientists in a variety of fields, and has been under intense investigation since Bjerrum first introduced the concept in the early part of this century.^{1–3} Much of what is known or conjectured concerning ion pairs is the result of measuring electrical and colligative properties of ion pair-containing solutions.⁴ However, as spectroscopic methods, particularly magnetic resonance techniques, have become more sophisticated, it has become possible to obtain more direct information concerning the structure and dynamics of ion pairs.^{5–10} We have previously described the use of steady-state $^1\text{H}\{^1\text{H}\}$ nuclear Overhauser effects (NOEs) to characterize the time-average structure of tetraalkylammonium tetrahydridoborate (R_4N^+ , BH_4^-) ion pairs in nonpolar solvents.^{11,12} This structure places the BH_4^- anion in a trigonal pyramidal site created by three alkyl chains of the tetraalkylammonium ion, and shows close

contact between the anion and the protons on the methylene group adjacent to the quaternary nitrogen of the cation. We also used steady-state $^{11}\text{B}\{^1\text{H}\}$ and $^{10}\text{B}\{^1\text{H}\}$ NOEs as well as ^{10}B and ^{11}B relaxation measurements to characterize the motions of the BH_4^- anion in these ion pairs.¹² We found that in solutions of tetrabutylammonium tetrahydridoborate (**1a**) in CDCl_3 , the anion reorients rapidly ($\tau_c \sim 10^{-12}$ s) relative to the overall motion of the ion pair. Furthermore, anion reorientation is sufficiently fast to average the local electrical environment, suppressing quadrupolar relaxation of the boron nucleus to a large extent. ^{10}B and ^{11}B relaxations for **1a** do not show significant differences when measured in nonpolar and dissociative solvents (such as water), so ion pairing does not appear to significantly affect the electronic environment of the boron.¹²

The motion of the cation, as well as the overall motion of the ion pair, is somewhat more complicated. The results of interionic NOE measurements for **1a** and for the related compounds tetraisoamylammonium tetrahydridoborate (**1b**) and tetraoctylammonium tetrahydridoborate (**1c**) in chloroform over a range of temperatures suggested to us that these ion pairs aggregate in nonpolar solution.¹³ NMR self-diffusion measurements performed with solutions of **1a** in CDCl_3 support the conclusion that ion pairs formed by **1a** aggregate in chloroform and also confirm that the ion aggregate is the primary diffusing species.¹⁴ Self-diffusion measurements for tetrabutylammonium chloride (**1d**) permitted us to estimate aggregate size by comparing the self-diffusion of the cation to that of a nonionic internal reference of similar shape and nominal mass, tetrabutylsilane (**2**).¹⁴ Similar estimates were made for **1a** as well.¹⁵

The present work is aimed at characterizing the motions of the tetrabutylammonium (TBA^+) cation and ion aggregates in

[†] Current address, General Electric Inc., Waterfront, NY.
[‡] Current address, Bruker Instruments, Inc., Billerica, MA.
[⊗] Abstract published in *Advance ACS Abstracts*, November 15, 1997.
 (1) Bjerrum, N. K. *Dan. Vidensk. Selsk.* **1926**, 7, No. 9.
 (2) Szwarc, M. *Ions and ion pairs in organic reactions*; Wiley-Interscience: New York, NY, 1972 and 1974; Vols. 1 and 2.
 (3) Reichardt, C. *Solvents and Solvent Effects in Organic Chemistry*, 2nd ed.; VCH: Weinheim, 1988.
 (4) Copenhaver, D. T.; Kraus, C. A. *J. Am. Chem. Soc.* **1951**, 73, 4557.
 (5) Grutzner, J. B.; Lawlor, J. M.; Jackman, L. M. *J. Am. Chem. Soc.* **1972**, 94, 2306.
 (6) Chen, N.; Witton, P. J.; Holloway, C. E.; Walker, I. M. *J. Coord. Chem.* **1988**, 19, 113.
 (7) Honeychuck, R. V.; Hersh, W. H. *J. Am. Chem. Soc.* **1989**, 111, 6056.
 (8) Kessler, H.; Feigel, M. *Acc. Chem. Res.* **1982**, 15, 2.
 (9) Miller, J. M.; Clark, H. H. *J. Chem. Soc., Chem. Commun.* **1982**, 1318.
 (10) Radley, K. *Mol. Cryst. Liq. Cryst., Lett. Sect.* **1989**, 6, 203.
 (11) Pochapsky, T. C.; Stone, P. M. *J. Am. Chem. Soc.* **1990**, 112, 6714–6715.
 (12) Pochapsky, T. C.; Wang, A.-P.; Stone, P. M. *J. Am. Chem. Soc.* **1993**, 115, 11084–11091.

(13) Stone, P. M.; Pochapsky, T. C.; Callegari, E. *J. Chem. Soc., Chem. Commun.* **1992**, 178–179.

(14) Pochapsky, S. S.; Mo, H.; Pochapsky, T. C. *J. Chem. Soc., Chem. Commun.* **1995**, 2513–2514.

(15) Mo, H.; Pochapsky, T. C. *J. Phys. Chem. B* **1997**, 101, 4485.

Table 1. Self-Diffusion Coefficients D Determined in CDCl_3 at 298 K by Pulsed Field Gradient NMR Experiments As Described in Refs 14 and 15 for Salts **1a**, **1d** and **1e**^a

compd (concn, M)	ion	D ($\times 10^{-10}$ m ² /s)	N
1a (0.2)	BH_4^-	5.34 ± 0.22	4.2
1a (0.2)	TBA^+	4.99 ± 0.14	5.2
1d (0.09)	TBA^+	6.20 ± 0.11	3.5
1e (0.08)	TBA^+	$8.6 \pm .2$	
1e (0.08)	acetate	8.1	

^a Aggregation numbers N are calculated as the inverse cube of the ratio of diffusion coefficients of the aggregating species and internal reference tetrabutylsilane (**2**). Detailed descriptions of experiments are given in refs 14 and 15. Errors are calculated from the maximum deviations of diffusion coefficients calculated by using individual resonances to the average coefficient for the molecule.

solutions of **1a** and **1d** in nonpolar solvents. To accomplish this, we fit the temperature dependence of homonuclear interionic NOEs using Solomon's theoretical treatment, assuming a single aggregate size.¹⁶ We have also measured $^{13}\text{C}\{^1\text{H}\}$ and $^{15}\text{N}\{^1\text{H}\}$ NOE and ^{15}N and ^{13}C nuclear relaxation parameters in ion pairs formed by the tetrabutylammonium ion, and analyze these data using a simplified version of the model-free approach of Lipari and Szabo.^{18,19} Finally, we analyze $^{29}\text{Si}\{^1\text{H}\}$ NOE, $^{13}\text{C}\{^1\text{H}\}$ NOE, and ^{13}C relaxation data for the reference compound tetrabutylsilane (**2**) to obtain an estimate of aggregate size independent of that obtained from NMR self-diffusion measurements.

Results and Discussion

General Considerations. Both the tetrahydridoborate **1a** and chloride **1d** salts of TBA^+ were used in the work described here. Cl^- and BH_4^- have the same charge and similar ionic radii (1.9 Å for BH_4^- and 1.81 Å for Cl^-). Both have advantages and disadvantages for the present studies. Samples of **1a** have limited lifetimes in CDCl_3 due to decomposition of BH_4^- , whereas samples of **1d** in chloroform can be prepared and stored in sealed tubes indefinitely. ^{35}Cl and ^{37}Cl have deficiencies as NMR probes, and the sensitivity of the interionic $^1\text{H}\{^1\text{H}\}$ NOE makes BH_4^- by far the preferred counterion for TBA^+ in experiments where interionic contacts or reorientations of interionic vectors are to be examined. Nevertheless, there is some indication (see Table 1) that at similar concentrations and temperature, **1a** aggregates to a somewhat greater extent than **1d**, and some caution is required when making comparisons between results obtained with the two salts.

Self-Diffusion of Ion Pairs. We have described the measurement of self-diffusion coefficients for ion pairs formed by **1a** and **1d** in CDCl_3 solution using pulsed field gradient-stimulated echo NMR experiments.^{14,15} Using tetrabutylsilane (**2**) as an internal reference, we showed that the aggregation of ion pairs formed by **1d** in CDCl_3 is primarily a response to solution crowding. Mean aggregate size increases with increasing **1d** concentration to an apparent maximum of ca. 4 ion pairs per aggregate over the concentration range we have studied (up to 0.1 M).¹⁴ Aggregation of **1d** shows little temperature dependence at a fixed concentration, indicating that aggregation is enthalpically neutral under these conditions. Because of sample stability considerations, temperature variation experiments were not performed for solutions of **1a** in CDCl_3 . However, the concentration dependence of diffusion for **1a** was similar to that of **1d**, so it is likely that similar thermodynamic considerations are valid in both cases.

The results of NMR self-diffusion measurements on **1a** and tetrabutylammonium acetate (**1e**) in CDCl_3 show that cation and

anion in both salts diffuse at similar rates in moderately concentrated solutions, as expected for tight ion pairs (see Table 1).¹⁵ However, only very small interionic NOEs are observed between the acetate methyl protons and cationic protons of **1e**. This indicates that the carboxylate group of the anion interacts most strongly with the tetrabutylammonium ion, and the methyl group of the acetate is relatively far from the cationic center. This is not surprising, since the driving force for ion pairing is mainly electrostatic. The similar self-diffusion coefficients for both the cation and anions of **1e** appear to rule out extensive solvent separation of the ions as the reason for this lack of interionic NOE.

Cation and Aggregate Dynamics from NOE and T_1 Relaxation. For a two-spin ($I = 1/2$) system, the steady-state NOE at spin I upon saturation of spin S may be expressed as:

$$\text{NOE} = f_I\{S\} = \frac{\gamma_S}{\gamma_I} \frac{\sigma_{IS}}{\rho_{IS} + \rho^*} \quad (1)$$

where σ_{IS} is the dipolar cross-relaxation rate constant and ρ_{IS} is the total dipolar relaxation rate constant for spin I . If relaxation pathways other than dipole–dipole (dd) exist, they attenuate the NOE, and are represented by ρ^* . The spin–lattice relaxation rate constant for spin I , R_{1I} , is given by:

$$R_{1I} = T_{1I}^{-1} = \rho_{IS} + \rho^* \quad (2)$$

Multiplication of eqs 1 and 2 yields:

$$\frac{\text{NOE}}{T_{1I}} = \frac{\gamma_S}{\gamma_I} \sigma_{IS} \quad (3)$$

Note that the expression on the right-hand side of eq 3 is also the $I\{S\}$ NOE buildup rate at short mixing times, which is linear with respect to the cross relaxation rate constant σ_{IS} . The dipolar relaxation rate constants ρ_{IS} and σ_{IS} are related to spectral densities and other experimental variables as follows:

$$\sigma_{IS} = \frac{1}{20} k^2 [6J(\omega_I + \omega_S) - J(\omega_I - \omega_S)] \quad (4)$$

$$\rho_{IS} = \frac{1}{20} k^2 [J(\omega_I - \omega_S) + 3J(\omega_I) + 6J(\omega_I + \omega_S)] \quad (5)$$

$$k = \frac{\mu_0}{4\pi} \gamma_I \gamma_S r_{IS}^{-3} \quad (6)$$

where μ_0 is the magnetic permeability of vacuum, r_{IS} is the internuclear distance between spins I and S , and the γ are the gyromagnetic ratios of the spins.^{16,17}

If the overall motion of the internuclear I – S vector is isotropic and can be described by a single correlation function, the spectral density $J(\omega)$ can be expressed as:

$$J(\omega) = \frac{2\tau_c}{1 + \omega^2\tau_c^2} \quad (7)$$

where τ_c is the overall correlation time. Combination of eqs 1–7 gives:

(17) Abragam, A. *Principles of Nuclear Magnetism*; Clarendon Press: Oxford, 1961.

(18) Lipari, G.; Szabo, A. *J. Am. Chem. Soc.* **1982**, *104*, 4546.

(19) Lipari, G.; Szabo, A. *J. Am. Chem. Soc.* **1982**, *104*, 4559.

(16) Solomon, I. *Phys. Rev.* **1955**, *99*, 559.

$$\text{NOE} = \frac{\gamma_S}{\gamma_I} \times \frac{\frac{6}{1 + (\omega_I + \omega_S)^2 \tau_c^2} - \frac{1}{1 + (\omega_I - \omega_S)^2 \tau_c^2}}{\frac{1}{1 + (\omega_I - \omega_S)^2 \tau_c^2} + \frac{3}{1 + \omega_I^2 \tau_c^2} + \frac{6}{1 + (\omega_I + \omega_S)^2 \tau_c^2} + \frac{10\rho^*}{k^2 \tau_c^2}} \quad (8)$$

$$T_{1I} = \frac{1}{\frac{1}{10} k^2 \tau_c} \times \frac{1}{\frac{1}{1 + (\omega_I - \omega_S)^2 \tau_c^2} + \frac{3}{1 + \omega_I^2 \tau_c^2} + \frac{6}{1 + (\omega_I + \omega_S)^2 \tau_c^2} + \frac{10\rho^*}{k^2 \tau_c^2}} \quad (9)$$

Equations 8 and 9 describe the relationship between the observables NOE and T_1 with the motional behavior represented by the correlation time τ_c , estimates for which are obtained by fitting experimental data. To accomplish this fit, reasonable values for k^2 and ρ^* are required. An *a priori* estimate of ρ^* is difficult to obtain, since by definition, multiple mechanisms may contribute to this rate constant and their origins may be quite complicated. The parameter k^2 is proportional to r_{IS}^{-6} . However, when dealing with large numbers of nuclei which may be contributing to the dipolar relaxation of the observed nucleus, the appropriate value of r_{IS} is not obvious, and both ρ^* and k must be treated as fittable parameters.

The fitting as described above also requires an assumption of isotropic motion in which one correlation time is sufficient for describing all motion in the system. The model-free formalism of Lipari and Szabo allows the consideration of more than one type of motion affecting relaxation.^{18,19} In this approach, the overall molecular motion is isotropic and characterized by a correlation time τ_c , while the motion of the internuclear I - S vector has an effective correlation time τ_{eff} . The local motion is described by τ_{eff} , which correlates to some extent with τ_c . The order parameter s is used to represent this correlation, with $s = 1$ representing complete correlation ($\tau_c = \tau_{\text{eff}}$) while $s = 0$ indicates that the local motion is completely uncorrelated with the overall motion of the molecule. (Situations where $s = 0$ are expected to be rare intramolecularly, but might apply in the present case when considering the relationship between the motion of the ion aggregate and the BH_4^- anion, which appears to be uncorrelated, see ref 12.) According to this approach,

$$J(\omega) = 2 \left(\frac{s^2 \tau_c}{1 + \omega^2 \tau_c^2} + \frac{(1 - s^2) \tau}{1 + \omega^2 \tau^2} \right) \quad (10)$$

where $\tau^{-1} = \tau_c^{-1} + \tau_{\text{eff}}^{-1}$.

If internal motion is very fast compared with overall orientation of the molecule, in the limit of $\tau_{\text{eff}} \rightarrow 0$ and s not very small, $J(\omega)$ can be simplified as:¹⁸

$$J(\omega) = 2 \frac{s^2 \tau_c}{1 + \omega^2 \tau_c^2} \quad (11)$$

This result differs from eq 7 by only a factor of s^2 , which means that fast internal motion makes dipolar relaxation less efficient.

Now combining eqs 7–9 and 11 gives the following expressions for the NOE and T_1 with s^2 included:

$$\text{NOE} = \frac{\gamma_S}{\gamma_I} \times \frac{\frac{6}{1 + (\omega_I + \omega_S)^2 \tau_c^2} - \frac{1}{1 + (\omega_I - \omega_S)^2 \tau_c^2}}{\frac{1}{1 + (\omega_I - \omega_S)^2 \tau_c^2} + \frac{3}{1 + \omega_I^2 \tau_c^2} + \frac{6}{1 + (\omega_I + \omega_S)^2 \tau_c^2} + \frac{10\rho^*}{k^2 s^2 \tau_c^2}} \quad (12)$$

$$T_1 = \frac{1}{\frac{1}{10} k^2 s^2 \tau_c} \times \frac{1}{\frac{1}{1 + (\omega_I - \omega_S)^2 \tau_c^2} + \frac{3}{1 + \omega_I^2 \tau_c^2} + \frac{6}{1 + (\omega_I + \omega_S)^2 \tau_c^2} + \frac{10\rho^*}{k^2 s^2 \tau_c^2}} \quad (13)$$

Phenomenologically, eqs 12 and 13 are equivalent to eqs 8 and 9, with $k^2 s^2$ replacing k^2 . For the purposes of data analysis we rewrite eqs 12 and 13 as:

$$\text{NOE} = \frac{\gamma_S}{\gamma_I} \frac{\frac{6}{1 + (\omega_I + \omega_S)^2 \tau_c^2} - \frac{1}{1 + (\omega_I - \omega_S)^2 \tau_c^2}}{\frac{1}{1 + (\omega_I - \omega_S)^2 \tau_c^2} + \frac{3}{1 + \omega_I^2 \tau_c^2} + \frac{6}{1 + (\omega_I + \omega_S)^2 \tau_c^2} + \frac{c_1}{\tau_c}} \quad (14)$$

$$T_1 = \frac{c_2}{\tau_c} \frac{1}{\frac{1}{1 + (\omega_I - \omega_S)^2 \tau_c^2} + \frac{3}{1 + \omega_I^2 \tau_c^2} + \frac{6}{1 + (\omega_I + \omega_S)^2 \tau_c^2} + \frac{c_1}{\tau_c}} \quad (15)$$

The ratio of the two expressions eliminates the leakage term c_1/τ_c :

$$\frac{\text{NOE}}{T_1} = \frac{\tau_c \gamma_S}{c_2 \gamma_I} \left(\frac{6}{1 + (\omega_I + \omega_S)^2 \tau_c^2} - \frac{1}{1 + (\omega_I - \omega_S)^2 \tau_c^2} \right) \quad (16)$$

The ratio NOE/ T_1 provides information concerning the cross relaxation rate between I and S . For small molecules in nonviscous solvents, the extreme narrowing limit ($\omega^2 \tau_c^2 \ll 1$) holds, and NOE/ T_1 is directly proportional to τ_c . As the temperature is lowered, the correlation time becomes longer and the absolute value of NOE/ T_1 becomes larger. However, once the system begins to move away from the extreme narrowing limit, the factors containing the inverse $\omega^2 \tau_c^2$ terms become important, and the absolute value of NOE/ T_1 decreases. Therefore, as a system moves from the extreme narrowing limit into a broadening regime, a maximum or minimum in the curve of NOE/ T_1 versus τ_c (or temperature) is expected, depending on relative signs of the gyromagnetic ratios of the spins involved. This phenomenon is observed for ion pairs discussed here (vide infra).

Aggregation Effects on Interionic Steady State $^1\text{H}\{^1\text{H}\}$ NOEs: Evaluation of Aggregate Rotational Correlation Times. We previously reported that steady-state interionic BH_4^- - $\{1\text{-CH}_2\}$ NOEs observed for ion pair **1a** and related ion pairs in CDCl_3 are profoundly temperature sensitive. As the temperature is decreased from 298 K the observed NOE becomes smaller, finally becoming zero around 223 K in a 7.05

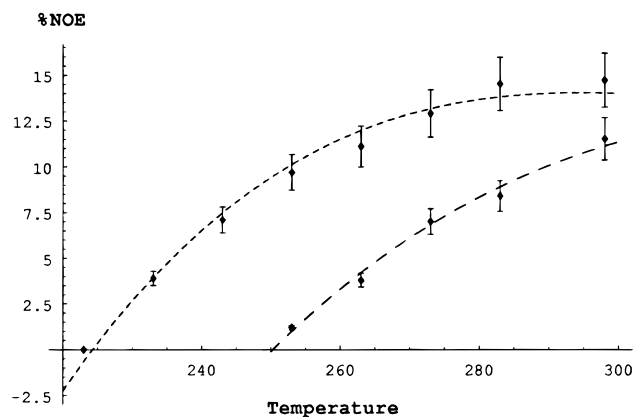


Figure 1. Nonlinear fit of steady-state interionic BH_4^- - $\{1\text{-CH}_2\}$ NOEs observed as a function of temperature for 0.2 M **1a** in CDCl_3 as described in refs 12 and 13. Coarse dashed line fits data obtained at 11.74 T, and fine dashed line fits data obtained at 7.05 T. Best-fit values of parameters NA and c_1 are shown in Table 2.

T field (300 MHz ^1H).¹³ Because the observed interionic NOEs deviate from what is predicted from eq 8 on the basis of the estimated correlation time of a single ion pair, it was concluded that ion pairs of type **1** aggregate in CDCl_3 , at least at low temperatures and moderate concentrations (0.2 M), with $\omega\tau_c \approx 1.12$ at 223 K. At that time, we made no attempt to fit the interionic NOE data to eq 8, as we assumed that average aggregate size would change as a function of temperature. However, the observation from self-diffusion measurements that the apparent aggregation state of ion pair **1d** is little affected by temperature, but appears to be almost completely a response to increasing concentration, has made it reasonable to attempt to fit the homonuclear interionic NOE to a single aggregate size.¹⁴ Before data analysis was begun, a complementary steady-state BH_4^- - $\{1\text{-CH}_2\}$ NOE data set was obtained at 11.74 T (500 MHz ^1H). The higher field changes the value of $\omega\tau_c$ at a particular temperature for a given sample and improves confidence in the fitting routine (vide infra). The results of both experimental runs are shown in Figure 1.

To incorporate aggregate size into an expression for the steady-state NOE (or for nuclear spin relaxation), a relationship is needed between aggregation state and the rotational correlation time, τ_c . The Stokes–Einstein equation is commonly used for predicting the correlation time as a function of experimental parameters:

$$\tau_s = 4\pi\eta r^3/3kT \quad (17)$$

where η is the viscosity of the solution, r is the radius of the molecule, k is Boltzmann's constant, and T is the absolute temperature. It has been found that the correlation time predicted by eq 17 (referred to hereafter as τ_s) is often larger than that measured experimentally, except for small polar molecules.²⁰ To adjust for such discrepancies in our fitting of the $^1\text{H}\{^1\text{H}\}$ NOE data for **1a**, we multiply τ_s by a correction factor A . A is expected to be a number not far from unity and a constant for molecules of similar size and shape (such as **1a** and **2**), and will also correct for any inaccuracies in the value used for the molecular radius r . We also assume that the volume of the aggregate increases linearly with aggregation number, N . This is justified by noting that the correlation time is directly proportional to the volume of a spherical species. In this case, the overall correlation time of the aggregate will be N times that of the monomer, assuming no interpenetration of the

Table 2. Values of NA and c_1 Obtained from Nonlinear Least-Squares Fitting of Experimental NOE Data for Interionic BH_4^- - $\{1\text{-CH}_2\}$ NOEs Observed for **1a** As Shown in Figure 1

B_0 (T)	NA	c_1 (s)
7.05	2.39 ± 0.05	$(2.6 \pm 0.1) \times 10^{-9}$
11.74	2.45 ± 0.05	$(1.7 \pm 0.1) \times 10^{-9}$

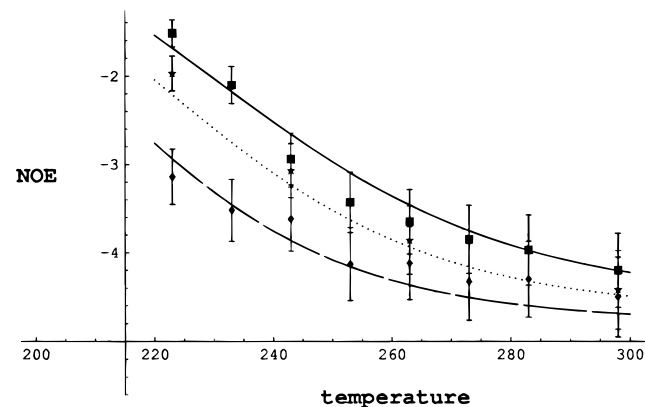


Figure 2. Nonlinear fit of steady-state $^{15}\text{N}\{^1\text{H}\}$ NOEs observed as a function of temperature for 0.2 M ^{15}N -labeled **1d** in CDCl_3 . Errors bars define 10% error in the observed data. Fit was obtained simultaneously for data at all field strengths. The coarse dashed line fits data obtained at 7.05 T (diamonds), the fine dashed line fits data obtained at 9.39 T (stars), and the solid line connects data obtained at 11.74 T (squares). Best-fit values of parameters are $NA = 3.81 \pm 0.14$ and $c = 2 \times 10^{-13}$ s/(rad \cdot T 2), where $cB_0^2 = \text{CSA}$ as explained in the text.

monomers. The corrected correlation time, including the correction for aggregation, is:

$$\tau_c = NA4\pi\eta r^3/3kT = NA\tau_s \quad (18)$$

Assuming a monomeric radius of 5 Å for ion pair **1a**, and using experimentally determined values for solvent viscosity,²¹ the interionic BH_4^- - $\{1\text{-CH}_2\}$ NOEs observed at two field strengths, 7.05 and 11.74 T, were fitted to eq 14 by varying NA and c_1 , the best-fit values of which are listed in Table 2. Experimental data and fitted curves are shown in Figure 1. It can be seen from Table 2 that similar NA values are obtained at both magnetic field strengths. Two conclusions can be reached from this. First, the data are well fit with a single value of NA (see Figure 1), so the aggregation number does not appear to change significantly as a response to temperature. Secondly, if A is a number near 1, the mean aggregate size is unlikely to be very large. Both of these conclusions are in agreement with those reached on the basis of our diffusion measurements on **1a** and **1d** in CDCl_3 . c_1 is also similar at both field strengths, and an explicit field dependent term was not required to obtain a good fit for this parameter. This is not true for relaxation and NOE involving ^{15}N in the ion pairs under study here (vide infra).

Overall Cation Reorientation: ^{15}N - and ^{29}Si - $\{^1\text{H}\}$ NOE and T_1 Measurements for **1d and **2**.** The reorientation of any internuclear vector through the central nitrogen of the tetrabutylammonium ion correlates strongly with the overall τ_c for the cation. Relaxation and NOE parameters for ^{15}N are therefore expected to report on the rotational motion of the cation. We synthesized ^{15}N -labeled **1d** and performed a series of steady-state $^{15}\text{N}\{^1\text{H}\}$ NOE and ^{15}N T_1 measurements as a function of temperature and magnetic field intensity. Steady-state $^{15}\text{N}\{^1\text{H}\}$ NOE was obtained by broad-band presaturation of ^1H , and ^{15}N T_1 values were measured with the inversion recovery method.

(20) Gierer, A.; Wirtz, K. Z. *Naturforsch. A* **1953**, 8, 532.

(21) Phillips, T. W.; Murphy, K. J. *Chem. Eng. Data* **1970**, 15, 304.

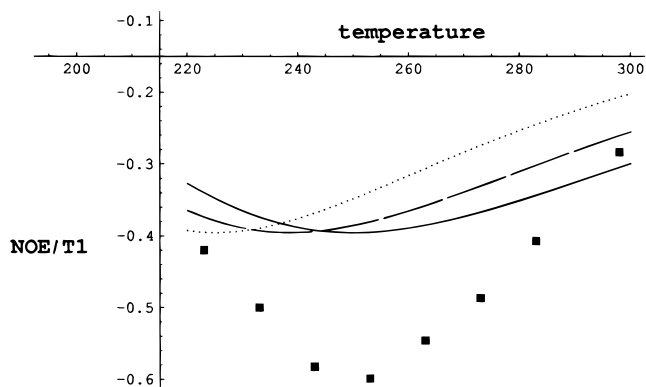


Figure 3. Plot of eq 16 for $^{15}\text{N}\{\text{H}\}$ NOE/ ^{15}N T_1 expected at 11.74 T for ion pair **1d** in CDCl_3 as a function of temperature for three values of NA at an arbitrary value of c_2 . Calculations were performed as described in the text assuming that NA is independent of temperature. The dotted line (\cdots) is for $NA = 1.5$, the broken line is for $NA = 2$, and the solid line is for $NA = 2.5$, the best fit value. For comparison, the experimental values of the ratio measured at 11.74 T are shown as filled squares.

To analyze the results of ^{15}N experiments, it was necessary to use a two-spin approximation, treating all of the protons in the molecule as a single nucleus. If ^1H is not decoupled during relaxation, the ^{15}N spin-lattice relaxation (T_1) is biexponential: one rate constant being $\rho_{IS} + \sigma_{IS}$ and the other being $\rho_{IS} - \sigma_{IS}$. Considering the fact that ρ_{IS} is at least twice σ_{IS} , and that ρ^* does not contribute to the cross-relaxation rate σ_{IS} , we assume that the rate of T_1 relaxation is $\rho_{IS} - \rho^*$ so that a single exponential rate constant may be used to describe this process. For this reason, the value of T_1 calculated by using a single exponential fit is expected to have $\sim 10\%$ error. In fact, a single exponential fit works quite well in the present case. $^{15}\text{N}\{\text{H}\}$ NOE buildup experiments were also performed to provide an independent estimate of the weighted average N-H distance $\langle r_{\text{NH}}^{-3} \rangle$ for calculating σ_{IS} .

Interestingly, an explicit magnetic field dependence for c_1 is required for fitting the steady state $^{15}\text{N}\{\text{H}\}$ NOE. At a given temperature, ^{15}N T_1 decreases with increasing field strength, and the magnitude of the NOE (which is negative in sign) also decreases with increasing field strength. This field dependence suggests that chemical shift anisotropy (CSA) provides an alternate pathway for ^{15}N T_1 relaxation. This is intriguing in that, although CSA is often an important mechanism for ^{15}N T_1 relaxation, it might not be expected to contribute significantly in the present case since the TBA^+ cation is symmetric. For example, $\Delta\sigma$ for the ammonium ion in the solid state is 0.²² One likely explanation for the observed field dependence of ^{15}N T_1 relaxation is that the Cl^- anion is bound in one of the trigonal pyramidal sites provided by the TBA^+ cation with a mean lifetime long enough to induce anisotropy in the local environment of the ^{15}N nucleus. The CSA is included in the calculations by assuming that it is the only contributor to ρ^* , and replacing ρ^* with cB_0^2 in which B_0 is the magnitude of field strength and c represents the magnitude of the CSA. The extreme narrowing limit is assumed to apply for ^{15}N CSA relaxation, which is dependent only on ω_N ($\tau_c < 10^{-10}$ s), and does not change over the temperature range studied. Figure 3 shows fitted experimental data for the $^{15}\text{N}\{\text{H}\}$ NOE at 7.05, 9.39, and 11.74 T, respectively. The data are best fit by using $NA = 3.81$.

Both $^{15}\text{N}\{\text{H}\}$ NOE and ^{15}N T_1 decrease in magnitude with decreasing temperature. However, the ratio NOE/ T_1 , which removes the field-dependent term c_1 from the fit, is more sensitive to the precise value of NA than the NOE term by itself. As τ_c increases with decreasing temperature, ρ_{IS} increases while σ_{IS} also increases at first, then begins to decrease, as expected from eq 16. As the system moves out of the extreme narrowing regime with increasing correlation time, the ratio NOE/ T_1 goes through a minimum (at least for ^{15}N , because of the negative sign of the gyromagnetic ratio). The position of the minimum is very sensitive to the value of NA used for the fit of NOE/ T_1 (see Figure 3). A value of $NA = 2.5$ gives the best fit to eq 16 for the position of the minimum as a function of temperature at all three fields (see Figure 3). However, the data at the extremes of temperature are not well fit to eq 16, particularly at 11.74 T. The assumption of an inverse temperature dependence of NA improves the fit, so it is possible that there is a small favorable enthalpic contribution to aggregation of ion pairs formed by **1d** (see Figure 4, parts a-c), although such an effect is not observed in self-diffusion measurements for **1d**.¹⁴ So it may be that some other as yet unknown consideration is still missing from the analysis.

To extract an estimate of aggregation number N from the values of NA shown in Tables 2 and 3, a value of NA for a non-aggregating species of similar size and shape to the TBA^+ ion is needed. We measured $^{29}\text{Si}\{\text{H}\}$ NOE and ^{29}Si T_1 for tetrabutylsilane (**2**, 0.2 M in CDCl_3), which has the same shape and size as the tetrabutylammonium ion but is uncharged and so is expected to have an aggregation number of $N = 1$. To a first approximation, the motional behavior of interatomic vectors originating at the silicon atom of **2** and at the quaternary nitrogen in **1d** will have similar constraints. Steady-state $^{29}\text{Si}\{\text{H}\}$ NOEs observed for **2** at 11.74 T with use of broadband ^1H decoupling are essentially constant over the temperature range 253 K to 298 K (measured fractional enhancements of -2.35 at 253 K and -2.37 at 298 K), with a maximum theoretical enhancement of -2.52 . These values are consistent with an $NA = 1.1 \pm 0.1$ for **2**, which, when compared to the corresponding $^{15}\text{N}\{\text{H}\}$ NOEs for **1d**, yields an aggregation number for **1d** of $N = 3.2 \pm 0.2$, a value similar to that obtained from diffusion measurements (see Table 1). A comparison of NOE/ T_1 for **1d** and **2** is more problematic. ^{29}Si T_1 relaxation for **2** is quite long, ranging from 44 s at 298 K to 12 s at 253 K, and the measurement is difficult due to the insensitivity and low natural abundance of ^{29}Si . However, measurements of $^{13}\text{C}\{\text{H}\}$ NOE and ^{13}C T_1 for both **1d** and **2** provide alternate means of measuring aggregation (vide infra).

Local Motions of Alkyl Groups in 1d and 2: $^{13}\text{C}\{\text{H}\}$ -NOE and ^{13}C T_1 . In contrast to ^{15}N or ^{29}Si relaxation described in the previous section, in which protons are not directly bonded to the relaxing nuclei and other relaxation mechanisms might compete significantly, methylene ^{13}C relaxation in **1d** and **2** is dominated by dipolar interactions with the attached protons. Good fits of ^{13}C NOE/ T_1 are obtained for the relaxation of the 1- CH_2 (directly attached to the central heteroatom) with both compounds. Since broadband decoupling of ^1H was performed during the ^{13}C T_1 relaxation experiments, $T_1^{-1} = \rho_{IS}$ in theory.¹⁷ However, T_1 is still assumed to be subject to 10% experimental error.

Fitting NOE/ T_1 data for the 1- CH_2 methylene carbon of **1d** to eq 16 in a manner similar to that described in the previous section yielded the fits shown in Figure 5. The simplified Lipari-Szabo treatment was used for data fitting (see eq 11). The corresponding data for silane **2** gave a best fit value of $NA = 0.54$. Dividing this into the values of NA obtained for **1d**

(22) Gibby, M. G.; Griffin, R. G.; Pines, A.; Waugh, J. S. *Chem. Phys. Lett.* **1972**, *17*, 80.

(23) Harbison, G.; Herzfeld, J.; Griffin, R. G. *J. Am. Chem. Soc.* **1981**, *103*, 4752.

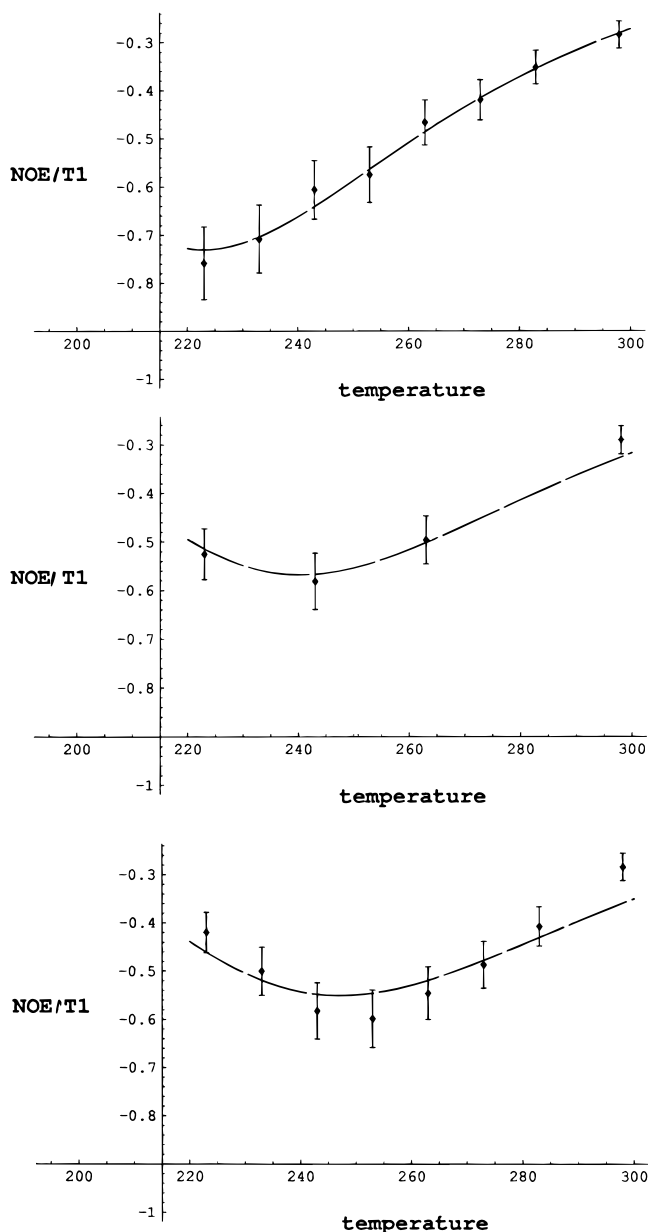


Figure 4. (a) Fit of $^{15}\text{N}\{^1\text{H}\}$ NOE/ ^{15}N T_1 measured at 7.05 T as a function of temperature for ion pair **1d** (0.2 M in CDCl_3). The fit was made assuming an inverse temperature dependence of N as described in the text. Values of NA and c_2 are shown in Table 3. (b) Fit of $^{15}\text{N}\{^1\text{H}\}$ NOE/ ^{15}N T_1 measured at 9.39 T as a function of temperature for ion pair **1d** (0.2 M in CDCl_3). The fit was made assuming an inverse temperature dependence of NA and c_2 as described in the text. Values of NA and c_2 are shown in Table 3. (c) Fit of $^{15}\text{N}\{^1\text{H}\}$ NOE/ ^{15}N T_1 measured at 11.74 T as a function of temperature for ion pair **1d** (0.2 M in CDCl_3). The fit was made assuming an inverse temperature dependence of NA as described in the text. Values of NA and c_2 are shown in Table 3.

Table 3. Values of NA and c_2 Obtained from Least-Squares Fitting of Experimental ^{15}N NOE/ T_1 Data Observed for **1d** As Shown in Figures 4a–c

B_0 (T)	NA		$c_2 \times 10^8$
	298 K	223 K	
7.05	1.77 ± 0.08	2.36 ± 0.08	2.07 ± 0.05
9.39	2.09 ± 0.14	2.80 ± 0.14	2.00 ± 0.06
11.74	2.07 ± 0.16	2.76 ± 0.22	1.66 ± 0.06

from the corresponding experiments yields an aggregation number of 3.2 ± 0.6 , the same as that calculated from the ^{15}N and ^{29}Si experiments described in the previous section.

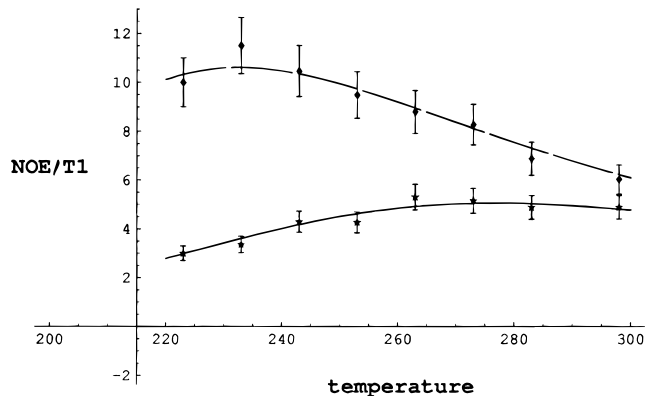


Figure 5. Fitting of NOE/ T_1 data for the 1- CH_2 methylene carbon of **1d** (0.2 M in CDCl_3) to eq 16. The dashed line fits data obtained at 7.05 T, the solid line connects data obtained at 11.74 T. Table 3 lists best-fit values of NA and c_2 .

Table 4. Values of NA and Fitting Constant c_2 Obtained from Nonlinear Least-Squares Fitting of ^{13}C NOE and Relaxation Data for 1- CH_2 Carbons of **1d** and **2**

compd	B_0 (T)	NA	$c_2 (\times 10^{10} \text{ s})$
1d	7.05	1.80 ± 0.09	3.63 ± 0.09
1d	11.74	2.38 ± 0.13	4.58 ± 0.01
2	7.05/11.74	0.54 ± 0.21	5.7 ± 2.0

Table 5. Correlation Times τ at 298 K for Various Types of Motion in Ion Pairs of Type **1** Shown in Figure 6^a

compd	type of motion	τ (ps)
1a	anion reorientation ^b	4
1d	effective for 1- CH_2 local motion	160
1d	overall cation/aggregate reorientation	260

^a Values of τ were calculated by using the values of NA obtained from nonlinear least-squares fitting of experimental NOE and relaxation data. ^b See ref 12 for complete description.

Discussion

The experimental data and analysis presented here provide insight into the molecular motions of cations and ionic aggregates in closed shell ion pairs formed in nonpolar solvents by lipophilic quaternary ammonium ions with small anions. Table 4 provides a summary of motional behavior in terms of correlation times calculated by using the values of NA determined here. Figure 6 provides a graphical representation of the types of independent motions which can occur.

Order parameters for the motion of the 1- CH_2 bond vectors in **1d** and **2** may be estimated by comparing best-fit values of NA calculated from ^{13}C NOE/ T_1 to those obtained from the ^{15}N and ^{29}Si relaxation parameters. The relaxation behavior of the central atom in each species reflects the overall correlation time of the ion pair (or aggregate) τ_c . In the simplified Lipari-Szabo treatment used here, the spectral density at the extreme narrowing limit which accounts for local motion is given by $s^2\tau_s$, where s is the order parameter correlating local motion to the overall motion of the molecule (see eq 11). Thus, the ratio of values of NA obtained for the same species from relaxation of the central atom (spectral density determined by τ_s) and the adjacent carbon atom (spectral density determined by $s^2\tau_s$) should yield an estimate for the order parameter. The ratio of the value of NA for **2** obtained from $^{29}\text{Si}\{^1\text{H}\}$ NOE to that obtained from the ^{13}C NOE/ T_1 for the same species is 0.6, yielding an order parameter of $s = 0.77$ for the local motion of the C–H bond in the 1-methylene of the silane. The corresponding calculation for ion pair **1d** with use of the values of NA obtained from $^{15}\text{N}\{^1\text{H}\}$ NOE yields an order parameter of

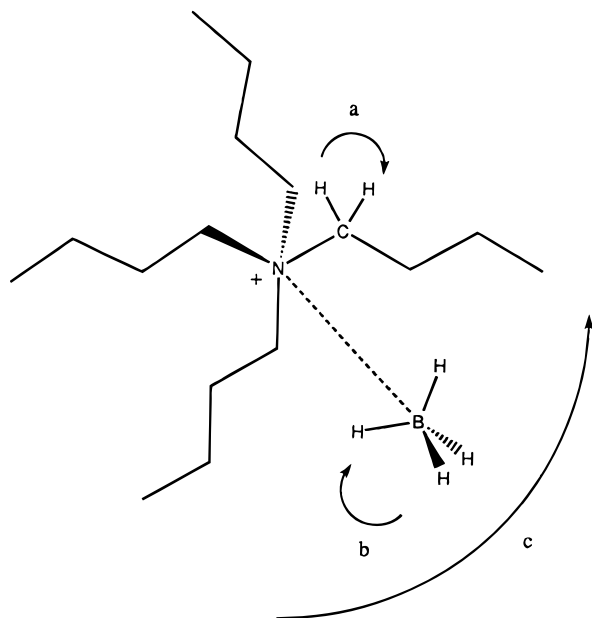


Figure 6. Types of motion in closed shell ion pairs of type **1**. (a) Local motion of bond vectors, reflected in the relaxation behavior of alkyl carbons. (b) Reorientation of the anion, reflected in ^{10}B and ^{11}B relaxation in **1a**. (c) Overall isotropic reorientation of the ion pair (or aggregate) reflected in the relaxation of the quaternary nitrogen and interionic NOE.

$s = 0.81$. The consistency of these values suggests that the observed differences in NA obtained by the various techniques are not an artifact of the analysis or the experiment, but reflect real differences in the types of motion being measured.

Comparison of Motional Correlation Times of the Aggregate, the Cation, and the Anion in **1a and **1d**.** Table 5 lists correlation times for various types of motion in ion pairs **1a** and **1d** based on the present results. In a previous publication, we described the use of ^{10}B and ^{11}B relaxation and $^{10}\text{B}\{^1\text{H}\}$ and $^{11}\text{B}\{^1\text{H}\}$ NOE to characterize the motional behavior of the BH_4^- anion in ion pairs formed by **1a** in CDCl_3 . Our conclusion from that work was that the anion was reorienting rapidly within a discrete binding mode (τ_c on the order of ps), averaging the electronic environment quickly enough to average out any electric field gradients due to the nearby cation, thereby suppressing the quadrupolar relaxation of both boron nuclides to a large extent. The observation of a field dependence for ^{15}N relaxation at the nominally symmetric quaternary ammonium nitrogen suggests that some residual chemical shift anisotropy exists in the tight ion pair. Given that anisotropies even for nonsymmetric quaternary ammonium ions are very small ($\Delta\sigma \approx 10$ ppm, see ref 23), it is unlikely that the anisotropy introduced by the presence of the anion is larger than 100 ppm. When this number is used to estimate a slow-exchange limit at 11.74 T, the lifetime of the chloride anion occupying a discrete binding mode is probably longer than 10^{-5} s, since CSA is incompletely averaged on the time scale of relaxation processes. This reduces the range of discrete binding mode lifetimes considerably from our earlier range of between 10^{-8} and 10^{-2} s. These previous estimates were based on the dominance of the correlation time of the aggregate upon the sign and intensity of the interionic $^1\text{H}\{^1\text{H}\}$ NOE for **1a**, the absence of differential relaxation effects between ^{10}B and ^{11}B in the same samples, and the observation of only averaged chemical shifts for all species in these studies.¹² If these new range estimates are correct, then this suggests that the structure and dynamics of discrete binding modes are important considerations in determining the outcome of reactions involving

closed shell ion pairs of this type, since the lifetimes of these discrete ion binding modes are long relative to bond-making and bond-breaking processes. In this light, the study of ion pair solution structure is particularly relevant when considering the mechanism of phase-transfer reactions and selective phase transfer catalyst design.

The general agreement between the aggregation numbers calculated by NMR diffusion experiments and those calculated with relaxation data supports our earlier conclusions that aggregate size is limited to less than five ion pairs even in the fairly concentrated solutions of ion pairs used in these experiments. This is not in agreement with the rather large aggregate sizes for these types of ion pairs calculated with freezing point depression methods.⁴ Furthermore, although self-diffusion is a translational phenomenon rather than rotational, the size of the aggregate formed appears to determine both rotational and translational motion, which suggests that the aggregates are roughly spherical, the shape for which both the diffusional and rotational forms of the Stokes–Einstein equation are best suited. We are currently preparing selectively labeled samples of **1d** to determine the time-average shapes of these ion aggregates using interionic NOEs.

Experimental Section

Synthesis of ^{15}N -Labeled **1d.** A 200-mg (3.67 mmol) sample of $^{15}\text{NH}_4\text{Cl}$ (CIL) was mixed with 5 mL of ethyl acetate, along with 2.7 g (14.7 mmol) of butyl iodide and 2.5 g (14.7 mmol) of 1,2,2,6,6-pentamethylpiperidine (PMP) in a 100-mL sealable bomb. The mixture was purged briefly with N_2 gas, and the bomb was sealed under N_2 . The reaction mixture was then heated to 90°C , and held there for 2 weeks. It was found to be critical that the reaction not be allowed to heat over 100°C , or byproducts were formed which rendered the purification more difficult. As the reaction proceeds, PMP hydroiodide salt and product precipitate from the reaction mixture. After cooling, the precipitate (which contains the product) was filtered and washed with a mixture of hexane and ethyl acetate to remove unreacted alkyl halide. The solid material was then washed three times with 5 mL of acetone, which selectively dissolves the product tetrabutylammonium iodide. After removal of the acetone by rotary evaporation, the crude product was recrystallized from hot water. The exchange of chloride for iodide was accomplished as described by Ford-Moore.²⁴ Into a 10-mL round-bottom flask was placed 0.92 g of AgNO_3 and 3 mL of distilled water. This solution was heated to boiling and 0.75 mL of concentrated hydrochloric acid was added dropwise with stirring. After the mixture was stirred for 30 min, the supernatant liquid was decanted, and the solid silver chloride was resuspended in 10 mL of distilled water and heated to 60°C . A solution of 0.8 g of the mixed tetrabutylammonium chloride/iodide was dissolved in 3 mL of methanol and added dropwise to the silver chloride. A yellow precipitate of AgI forms as the addition proceeds. The mixture was stirred at reflux for another hour and then allowed to cool with stirring for half an hour. The precipitate was filtered and washed with hot water, and the filtrate was concentrated under vacuum to yield a white solid, ^{15}N -**1d**. The completeness of the alkylation reaction and purity of the product were confirmed by NMR. The final yield was 15% of theoretical.

Synthesis of Tetrabutylsilane (2). Tetrabutylsilane (**2**) used in NMR experiments was either distilled from commercially available material (Lancaster) or prepared according to the method of Gilman and Clark.²⁵ Into a dry three-necked 25-mL round-bottom flask fitted with a condenser and N_2 inlet was added 3 mL of anhydrous diethyl ether. The flask was placed in an ice bath, and 5 mL (0.043 mol) of tetrachlorosilane (Petrarch) was introduced by syringe. Then, 65 mL of a 1.6 M butyllithium solution in diethyl ether (0.104 mol) was added dropwise with stirring. A white precipitate formed as addition continued. After addition was complete, the ice bath was removed and the reaction mixture brought to reflux and held there for 30 min.

(24) Ford-Moore, A. H. *Organic Synthesis*; John Wiley & Sons: New York, 1963; Collect. Vol. IV, p 84.

(25) Gilman, H.; Clark, R. N. *J. Am. Chem. Soc.* **1947**, *69*, 967.

After cooling, the reaction mixture was hydrolyzed by the addition of dilute HCl. The ether and water layers were separated, and the ether layer was washed once with 15 mL of concentrated H₂SO₄ and three times with 30 mL of water. The ether layer was dried over anhydrous sodium sulfate and concentrated under vacuum to yield a clear liquid. This liquid was fractionally distilled with use of a Vigreux column, and the fractions obtained between 85 and 145 °C were collected. This fraction was redistilled, and the fractions obtained between 120 and 145 °C were recollected. Purity of the product was confirmed by NMR.

NMR Spectroscopy. Experiments were performed on one of three instruments. The 7.05 T experiments were performed on a Varian XL-300 (Brandeis University) equipped with a broad band probe, the 9.39 T experiments were performed on a Bruker ARX-400 (Bruker Instruments, Billerica, MA), and the 11.74 T experiments were performed on a Bruker AMX-500 (Brandeis University). Both the ARX-400 and AMX-500 are equipped with broadband tunable probes. As a function of magnetic field strength (7.05, 9.39, and 11.74 T), ¹H resonates at 300, 400, and 500 MHz, respectively, ¹⁵N resonates at 30.4, 40.5, and 50.7 MHz, respectively, ¹³C resonates at 75.4, 100.6, and 125.7 MHz, respectively, and ²⁹Si resonates at 59.6, 79.5, and 99.3 MHz, respectively.

Sample Preparation. Samples were prepared for spectroscopy in CDCl₃ (Cambridge Isotopes Laboratories) that had been passed over activated neutral alumina to remove traces of acid. Tetrabutylammonium tetrahydridoborate was obtained from Aldrich, tested for purity by elemental analysis, and used without further purification. Samples to be used in NOE experiments were freeze-thaw degassed multiple times to remove traces of oxygen.

Steady State X{¹H} NOE. The experimental conditions for measurement of the selective interionic ¹H{¹H} NOE have been described previously.¹² Steady state heteronuclear NOEs were measured by using broadband composite pulse saturation of ¹H during a preacquisition delay time set to approximately five times the T₁ relaxation time in order to ensure steady state, followed by a read pulse on X and direct observation of the X nucleus with ¹H decoupling. Reference

spectra were obtained in a similar fashion, but without the ¹H presaturation. NOE was measured by integrating the signal intensity of the X resonance in the presence of ¹H saturation, subtracting the signal intensity without saturation, and dividing the difference by the signal intensity without saturation.

X T₁. Heteronuclear T₁ values were measured by using a standard inversion recovery sequence *delay-π-τ-π/2-acq*, where τ is the variable relaxation delay. Eight values of τ ranging from 0 to 2 s were used. For ¹⁵N and ²⁹Si T₁ measurements, ¹H decoupling is applied only during acquisition. For ¹³C T₁, ¹H decoupling was applied during the delay prior to the beginning of the sequence as well as during acquisition.

Data Fitting. All data fitting was performed as described in the text with use of the nonlinear regression analysis package available with Mathematica 3.0 (Wolfram, Inc.), and values of the fitting parameters obtained from these analyses were used to calculate the fitting curves shown in all figures. All plots of data and fitting curves were also prepared with use of Mathematica 3.0. Previously reported viscosity data²¹ for chloroform as a function of temperature were fit by using a linear least-squares routine in Mathematica 3.0 to yield the following expression:

$$\log \eta = -3.646 + 584.9t^{-1} + (7.22 \times 10^{-3})t - (8.26 \times 10^{-6})t^2$$

Values for chloroform viscosity calculated with use of this expression were then substituted into the fitting equation to obtain τ, as a function of temperature.

Acknowledgment. This work was supported in part by a grant from the NSF (CHE-9510131). T.C.P. also acknowledges support from the NSF Young Investigators Program (CHE-9257036) and the Camille and Henry Dreyfus Teacher-Scholar Program.

JA9723139